The Plant Cell, Vol. 19: 3791–3804, November 2007, www.plantcell.org

Structural and Functional Analysis of SGT1 Reveals That Its Interaction with HSP90 Is Required for the Accumulation of Rx, an R Protein Involved in Plant Immunity [W] [OA]

Marta Botër,[a,1] Béatrice Amigues,[b,1] Jack Peart,[a] Christian Breuer,[a] Yasuhiro Kadota,[c] Catarina Casais,[a] Geoffrey Moore,[d] Colin Kleanthous,[e] Francoise Ochsenbein,[b] Ken Shirasu,[a,c,2] and Raphaël Guerois[b,2]

[a] Sainsbury Laboratory, John Innes Centre, Norwich NR4 7UH, United Kingdom
[b] Commissariat à l'Energie Atomique (CEA), Institut de Biologie et Technologies de Saclay (IBITECS), and Centre National de la Recherche Scientifique (CNRS), Gif-sur-Yvette F-91191, France
[c] RIKEN Plant Science Center, Tsurumi-ku, Yokohama, 230-0045 Japan
[d] School of Chemical Sciences and Pharmacy, University of East Anglia, Norwich NR4 7TJ, United Kingdom
[e] Department of Biology, University of York, York YO10 5YW, United Kingdom

SGT1 (for suppressor of G2 allele of *skp1*) and RAR1 (for required for *Mla12* resistance) are highly conserved eukaryotic proteins that interact with the molecular chaperone HSP90 (for heat shock protein90). In plants, SGT1, RAR1, and HSP90 are essential for disease resistance triggered by a number of resistance (R) proteins. Here, we present structural and functional characterization of plant SGT1 proteins. Random mutagenesis of *Arabidopsis thaliana* SGT1b revealed that its CS (for CHORD-SGT1) and SGS (for SGT1 specific) domains are essential for disease resistance. NMR-based interaction surface mapping and mutational analyses of the CS domain showed that the CHORD II domain of RAR1 and the N-terminal domain of HSP90 interact with opposite sides of the CS domain. Functional analysis of the CS mutations indicated that the interaction between SGT1 and HSP90 is required for the accumulation of Rx, a potato (*Solanum tuberosum*) R protein. Biochemical reconstitution experiments suggest that RAR1 may function to enhance the SGT1–HSP90 interaction by promoting ternary complex formation.

INTRODUCTION

Higher plants have evolved a sophisticated pathogen surveillance system whereby pathogen effectors are detected, directly or indirectly, by a repertoire of resistance (R) proteins (Jones and Dangl, 2006). The recognition of pathogen effectors by these R proteins activates a common defense mechanism known as hypersensitive response, which includes the oxidative burst, the induction of defense-related genes, and localized cell death, suggesting the convergence of signaling pathways (Shirasu and Schulze-Lefert, 2000). Currently, little is known about how R proteins transduce signals to downstream components.

Recent genetic and inhibitor studies revealed that many R proteins that contain nucleotide binding site (NBS) and leucine-rich repeat (LRR) domains require heat shock protein90 (HSP90) for function (Hubert et al., 2003; Kanzaki et al., 2003; Takahashi et al., 2003; Liu et al., 2004). HSP90 is a highly conserved molecular chaperone in eukaryotes that is essential for the maturation and activation of many signaling proteins, often referred to as clients. The general mechanism of protein maturation first involves the binding of the client to HSP90, potentially mediated by HSP70 (Pratt and Toft, 2003). The mature client is then released following a cell signal that is coupled to the hydrolysis of ATP by HSP90. The rate of ATP hydrolysis is thus critical for the fine-tuning of client maturation (Pratt and Toft, 2003; Pearl and Prodromou, 2006). The ATPase activity of HSP90 is regulated by transient interactions with a plethora of proteins named cochaperones that bind either HSP90 or HSP70 or both. Some cochaperones also associate with their specific clients. Hence, the key to unraveling the chaperoning process is dissection of the cooperative interactions between cochaperones and HSP90/HSP70 that can block or accelerate the ATP cycle and so regulate the recruitment of client proteins.

HSP90 interacts specifically with SGT1 (for suppressor of G2 allele of *skp1*) and RAR1 (for required for *Mla12* resistance), which are major regulatory components of disease resistance triggered by many R proteins (Shirasu et al., 1999; Azevedo et al., 2002; Takahashi et al., 2003). SGT1 and RAR1 are highly conserved eukaryotic proteins that interact with each other, but their precise roles in HSP90 function have remained elusive. Like HSP90, both SGT1 and RAR1 are required for the stabilization of many R proteins (Tornero et al., 2002; Bieri et al., 2004; Azevedo et al., 2006). Similarly, both HSP90 and SGT1 are required for the stabilization and assembly of the yeast CBF3 (for centromere

[1] These authors contributed equally to this work.
[2] Address correspondence to ken.shirasu@psc.riken.jp or raphael.guerois@cea.fr.
The authors responsible for distribution of materials integral to the findings presented in this article in accordance with the policy described in the Instructions for Authors (www.plantcell.org) are: Ken Shirasu (ken.shirasu@psc.riken.jp) and Raphaël Guerois (raphael.guerois@cea.fr).
[W] Online version contains Web-only data.
[OA] Open Access articles can be viewed online without a subscription.
www.plantcell.org/cgi/doi/10.1105/tpc.107.050427

binding factor3) and the human kinetochore complexes (Bansal et al., 2004; Lingelbach and Kaplan, 2004; Steensgaard et al., 2004; Niikura et al., 2006). As yeast does not contain any RAR1 homolog, CBF3 complex assembly is a RAR1-independent process. Whether CHP1, a RAR1 homolog in human, is required for the kinetochore complex assembly is not known, although the *Aspergillus* homolog CHPA seems not to be involved in this process (Sadanandom et al., 2004). Interestingly, SGT1 is also involved in degradative processes, as it is required for the function of several SCF (for SKP1/CULLIN1/F-box protein) complexes in *Saccharomyces cerevisiae* and plants (Kitagawa et al., 1999; Gray et al., 2003; Bansal et al., 2004). In these organisms, SGT1 interacts with SCF subunit SKP1, indicating its role in the degradation of a potentially large number of proteins. Thus, SGT1 may be a key regulator coupling the stabilization and degradation of proteins.

To elucidate the molecular mechanism of how R proteins function, it is critical to understand the complex interplay between domains of HSP90, SGT1, and RAR1. HSP90 is composed of three domains: an N-terminal domain (NTD) containing an ATP binding module, a middle client binding domain, and a C-terminal dimerization domain (Pearl and Prodromou, 2006). SGT1 is composed of three conserved regions: an N-terminal TPR (for tetratricopeptide repeat) domain, a central CS (for CHORD-SGT1) domain, and a C-terminal SGS (for SGT1-specific) domain (Azevedo et al., 2002). RAR1 is made up of two homologous zinc binding domains, CHORD I and CHORD II (Shirasu et al., 1999; Heise et al., 2007). The N-terminal domain of HSP90 (HSP90-NTD) and the CS domain of SGT1 are known to interact with the CHORD I and CHORD II domains of RAR1, respectively (Azevedo et al., 2002; Takahashi et al., 2003). Moreover, HSP90-NTD and the CS domain of SGT1 interact with each other in plants (Takahashi et al., 2003). Therefore, competition or synergy between RAR1 and SGT1 for binding HSP90 might occur either through the CS domain, interacting with both the HSP90-NTD and the CHORD II domains, or through HSP90-NTD, interacting with both the CHORD I and CS domains.

In this study, we combined genetic analysis and structure determination with biochemical and physiological assays to unravel the intricate network formed by SGT1, RAR1, and HSP90 in plant disease resistance. We used two similar copies of *Arabidopsis thaliana SGT1: SGT1a* and *SGT1b*, either of which can confer Rx-dependent resistance to *Potato virus X* (PVX) in a heterologous complementation system in *Nicotiana benthamiana* (Azevedo et al., 2006). The complementation assay with randomly mutagenized *SGT1b* revealed amino acid residues that are important for its function in Rx resistance. NMR spectroscopy was used to identify the surfaces of the CS domain involved in binding to HSP90-NTD and the CHORD II domain of RAR1. Targeted mutagenesis revealed that Rx-mediated resistance and Rx stabilization require SGT1–HSP90 association. In vitro binding assays showed that HSP90-NTD and CHORD II can bind simultaneously to the CS domain. By contrast, the CS domain and CHORD I were found to compete for binding to the HSP90-NTD domain. No competition was observed in the context of the full-length proteins; instead, the interaction between HSP90 and At SGT1b was greatly enhanced in the presence of RAR1. Together, these data support a mechanism in which the role of RAR1 may be to enhance the function of SGT1 on HSP90 by acting as a bridge between the two proteins.

RESULTS

Arabidopsis SGT1b CS and SGS Domains Are Required for Rx-Mediated Disease Resistance

To understand how SGT1 functions in disease resistance, we screened a series of randomly generated point mutations in At *SGT1b* for loss of function (LOF) in resistance against PVX conferred by a potato (*Solanum tuberosum*) R protein, Rx. To generate a mutant library, At *SGT1b* cDNA was mutagenized in vitro by error-prone PCR and cloned into a binary vector, pBin61 (Bendahmane et al., 2002) (Figure 1A). Mutants were screened for disease resistance using *N. benthamiana* that had been infected with PVX-GFP (for green fluorescent protein), and endogenous Nb *SGT1* was silenced (Azevedo et al., 2006). Transient expression of wild-type At *SGT1b* restores resistance and so prevents the accumulation of PVX-GFP in plants expressing *Rx* under the control of its own promoter. At *SGT1b* LOF mutants are expected not to complement the loss of Nb *SGT1*, allowing the accumulation of PVX-GFP to levels similar to those of the β-glucuronidase (GUS) control (thus susceptible) (Figure 1A). We tested 960 individual At *SGT1b* mutagenized clones and identified 281 putative LOF mutants. Immunoblot analyses of the protein extracts were then used to eliminate clones that were not able to express at the level of wild type SGT1b or that produced truncated derivatives (see Supplemental Figure 1 online). After bioassay and immunoblot analyses, 24 LOF clones were selected for further analyses. Sequencing of the LOF clones revealed that six contained a single mutation, but most contained two or more mutations. By splitting these mutations using chimeric PCR, we identified another 10 single LOF mutations. Of these 16 LOF single mutants, 5 were localized to the CS domain (CSb) and 11 to the SGS domain (SGSb) (Figures 1B and 2). No LOF mutation was found in the TPR domain (TPRb) or the variable regions of SGT1b. In summary, these results indicate that the CS and SGS domains of At SGT1b are essential for Rx resistance.

SGT1b Mutations for Dominant-Negative Effects in Disease Resistance

The At *SGT1b* mutant library was also screened for DN effects on Rx resistance against PVX. Overexpression of these mutants should interfere with Rx-mediated resistance, allowing more accumulation of PVX-GFP. In this case, plants would exhibit larger necrotic spots as indicative of PVX spreading (Figure 1A). Indeed, RNA gel blot analysis confirmed that leaves with larger necrotic spots accumulated more PVX mRNA (see Supplemental Figure 2 online). Using a strategy similar to the LOF screening, we tested 2400 randomly mutagenized clones and isolated 9 single causative mutations (Figures 1A and 1B). Three of these corresponded to LOF mutations bM319V, bK321E, and bE325V in the SGSb domain (Figure 2). Four other DN mutations, bS326L, bT329M, bV338A, and bP347* (frameshift), were also located in the SGSb domain, and two weak DN mutations were identified in

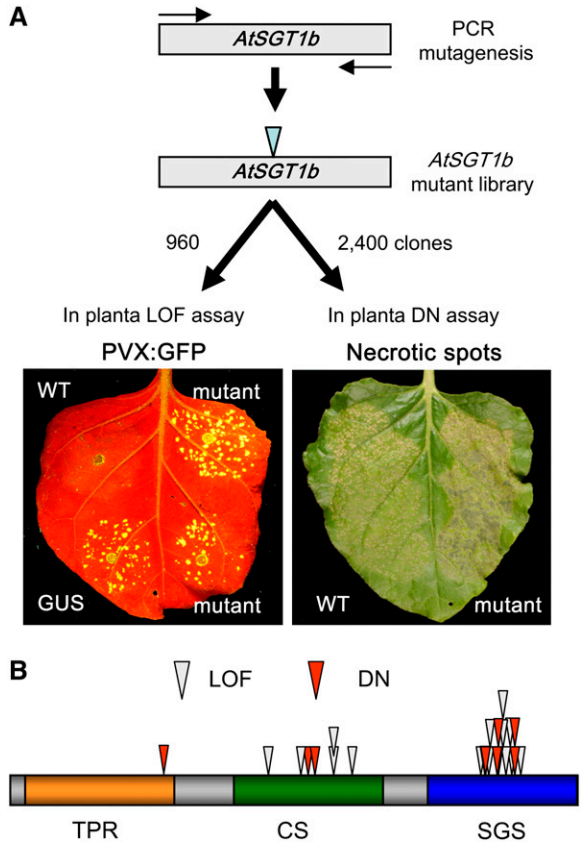

Figure 1. Mutations in At SGT1b Interfere with Its Function in Rx-Mediated Resistance against PVX.

(A) Screening strategy for LOF and dominant-negative (DN) mutations. The At *SGT1b* gene was mutated using error-prone PCR and then used for the *Agrobacterium tumefaciens*–based transient screening for LOF (left panel) and for DN effect (right panel) in Rx-mediated resistance against PVX. For the LOF assay, *Rx*-containing *N. benthamiana* plants silenced for Nb *SGT1* were coinfiltrated with *Agrobacterium* expressing At *SGT1b* mutants and *PVX-GFP* (right half of the leaves). For controls, wild-type At *SGT1b* (positive) and *GUS* (negative) were used (left half of the leaves). PVX accumulation was monitored by GFP fluorescence under UV illumination at 5 d after inoculation. For the DN assay, At *SGT1b* mutants were coexpressed with *Rx* and *PVX-GFP* by *Agrobacterium* infiltration in *N. benthamiana* wild-type plants. The appearance of necrotic spots was monitored at 5 to 7 d after inoculation.
(B) Schematic representation of LOF and DN mutations in At SGT1b. White and red triangles represent LOF and DN mutations, respectively.

the CSb domain (bG190D) in CSb and at the C-terminal end of TPRb (bE119G) (Figures 1B and 2). Two of the SGSb DN mutants, bT329M and bV338A, showed reduced functionality. We tested all of the LOF mutants for DN effects and found that the bQ166R mutation exhibited a very weak DN effect, while other CS mutants showed no DN effect. Interestingly, most of the LOF mutations in SGSb also had a DN effect, with the exception of bR316G.

Since both RAR1 and HSP90 bind SGT1, we investigated whether this binding capability was altered in LOF and DN mutants using a yeast two-hybrid assay (Figure 2). We found that all LOF mutations (bQ166R, bF189S, bC221R, bC221R, and bK229E) in CSb completely abolished the interaction with At HSP90.1. Four CSb mutants, bQ166R, bF189S, bC221R, and bC221Y, were also impaired in At RAR1 binding. The two DN mutants bE119G and bG190D were still able to interact with HSP90.1; however, only bE119G bound RAR1. None of the SGSb mutations affected RAR1 or HSP90.1 binding. These data indicate that the CSb domain of SGT1b is required for the interaction with both RAR1 and HSP90.

Solution Structure of the At SGT1b CS Domain

To understand how these mutations might affect the structure and function of the CS domain, we determined its solution structure by NMR. For this purpose, we used a glutathione *S*-transferase (GST) fusion protein with the CS domain of At SGT1a (CSa) expressed in *Escherichia coli*, because of its high solubility. The ^{1}H-^{15}N heteronuclear single quantum correlation (HSQC) spectrum of the CSa domain showed that cross-peaks, which correlate the frequencies of backbone and side chain amide nitrogen nuclei with those of their attached protons, were well defined and dispersed (see Supplemental Figure 3 online). From a series of triple resonance three-dimensional experiments, resonances arising from the backbone N, C, and H atoms were assigned together with those of the C^{β} and H^{β} nuclei. The secondary structures of CSa were inferred from the nuclei N, C^{α}, C^{β}, and H^{α} and chemical shifts using the TALOS program (Cornilescu et al., 1999), which yielded secondary structure maps very similar to those of the CS domain from human SGT1 (Lee et al., 2004). Since both *Arabidopsis* and human SGT1 sequences share ~38% identity in the region spanning the CS domain, we built a three-dimensional structure of the CSa domain using homology modeling (Figures 3A and 3B). Given the level of sequence identity, the structural model of the plant domain is likely to be very close (typically 2 to 3 Å) to the native structure, with differences located mainly in the loops (Ginalski, 2006). The sequences of CSa and CSb are sufficiently similar (74% identity) that their structures are likely to be nearly identical. The modeled structure of the CS domain is a β-sandwich made of seven antiparallel β-strands, with β-strands 1, 2, 6, and 7 on one face and β-strands 3, 4, and 5 forming the other face (Figure 3B). Two α-turns, α1 and α2, precede β-strands 3 and 6, respectively. This structural model confirms an early prediction that the CS domain is similar to the HSP90 cochaperone, P23 (Dubacq et al., 2002; Garcia-Ranea et al., 2002). Based on the CS structure, we found that bQ166, bF189, and bC221 are buried in the core of the domain and that these mutations are likely to be structurally disruptive (Figure 3B). On the other hand, residues bK229 and bG190 are exposed on the surface of the protein and likely cause changes in binding rather than folding.

The Nonconserved Surface of the CS Domain Binds the CHORD II Domain

Based on the structural model and resonance assignments, we mapped the region on CSa that interacts with the CHORD II domain of At RAR1 from complexation-induced perturbations to the ^{1}H-^{15}N HSQC spectrum. The ^{1}H-^{15}N HSQC experiment

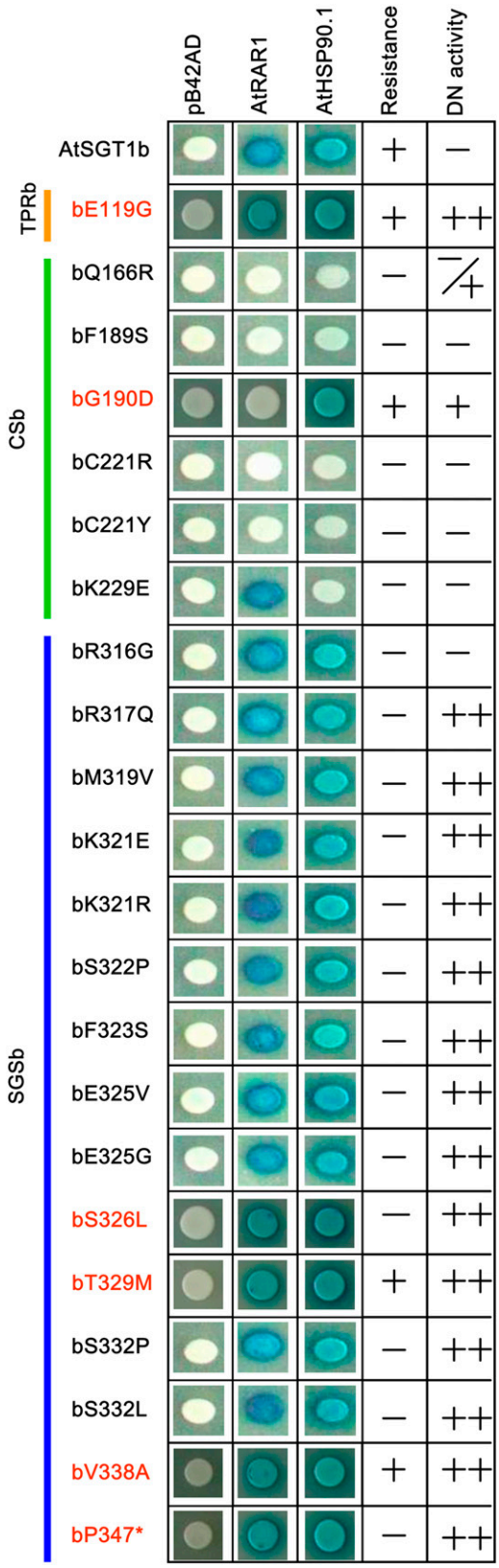

Figure 2. LOF and DN Mutations in At SGT1b.

At SGT1b LOF and DN mutants were assayed for interaction with At RAR1 and At HSP90.1 by the *lexA*-based yeast two-hybrid system. At *SGT1b* derivatives were cloned into pLexA (binding domain fusion) and At *RAR1* and At *HSP90.1* into pB42AD (activator domain fusion) vectors. Interactions were detected by induction of *lacZ* reporter genes under the control of the *lexA* gene in yeast EGY48 cells. The asterisk indicates a frameshift mutation. Resistance functions for Rx (+ as wild type, − as LOF) and DN activity (+ and ++ as DN, − as wild type) were assayed as in Figure 1. Mutations found in LOF and DN screenings are indicated in black and red, respectively.

provides a fingerprint of the protein structure whose cross-peaks are sensitive to any structural or environmental variation upon binding of a partner. The superimposed HSQC spectra of free CSa and CSa mixed with CHORD II in a 1:1 molar ratio show that the majority of resonances remain invariant (see Supplemental Figure 3B online). However, a limited set of cross-peaks disappeared and reappeared in another region of the spectrum, indicating that the free and bound forms are in slow exchange on the NMR time scale (slower than milliseconds). The most perturbed residues cluster in a region centering on the hairpin between β-strands 3 and 4 and β-strand 5, to which the hairpin is hydrogen-bonded (Figures 3B and 3C).

To further define the amino acids involved in the interaction, several point mutants of solvent-exposed residues were engineered into this hairpin in CSa and binding to full-length At RAR1 protein was monitored using pull-down assays. Figure 4A shows that mutations aG182D and aI185D disrupted the ability of CSa to bind to RAR1 in vitro. We next tested their interaction with HSP90; for this purpose, we used wheat (*Triticum aestivum*) HSP90 (Ta HSP90) because of its higher solubility in vitro. None of the mutations affected binding to Ta HSP90, indicating that the overall CS domain structure was not altered in the mutants. Indeed, ^{1}D NMR spectra of CSa aG182D and aI185D indicated that no major changes occurred in the structure of these domains (data not shown). These positions correspond to residues whose NMR signals were most affected upon CHORD II binding. By contrast, mutations aD180A and aE191K, located in the middle of β-strand 3 and at the end of β-strand 4, respectively, did not affect the binding of the CSa domain with CHORD II. Similarly, both aG182D in full-length SGT1a and its equivalent bG190D in SGT1b were not able to interact with RAR1 in vitro (Figure 4B). Thus CHORD II binds to a limited region in the turn connecting the two β-strands 3 and 4 of the CS domain. Comparison between the CHORD II binding region and the conservation index mapped upon the surface of CSa (see Supplemental Figure 4 online) shows that CHORD II binds to the nonconserved face of the CSa domain. This conclusion was also confirmed by yeast two-hybrid analysis (Figure 4C). We note that an interaction between barley (*Hordeum vulgare*) Hv HSP90 and SGT1a or aG182D could not be detected in these experiments. As the CSa domain alone binds tightly to full-length HSP90 (Figure 4A) and Hv HSP90-NTD alone binds to full-length SGT1a (Figure 4C), other domains likely hamper the interaction in the yeast two-hybrid experiment. It is likely that the interaction between SGT1a and HSP90 might be transient and/or require particular conformations in plants.

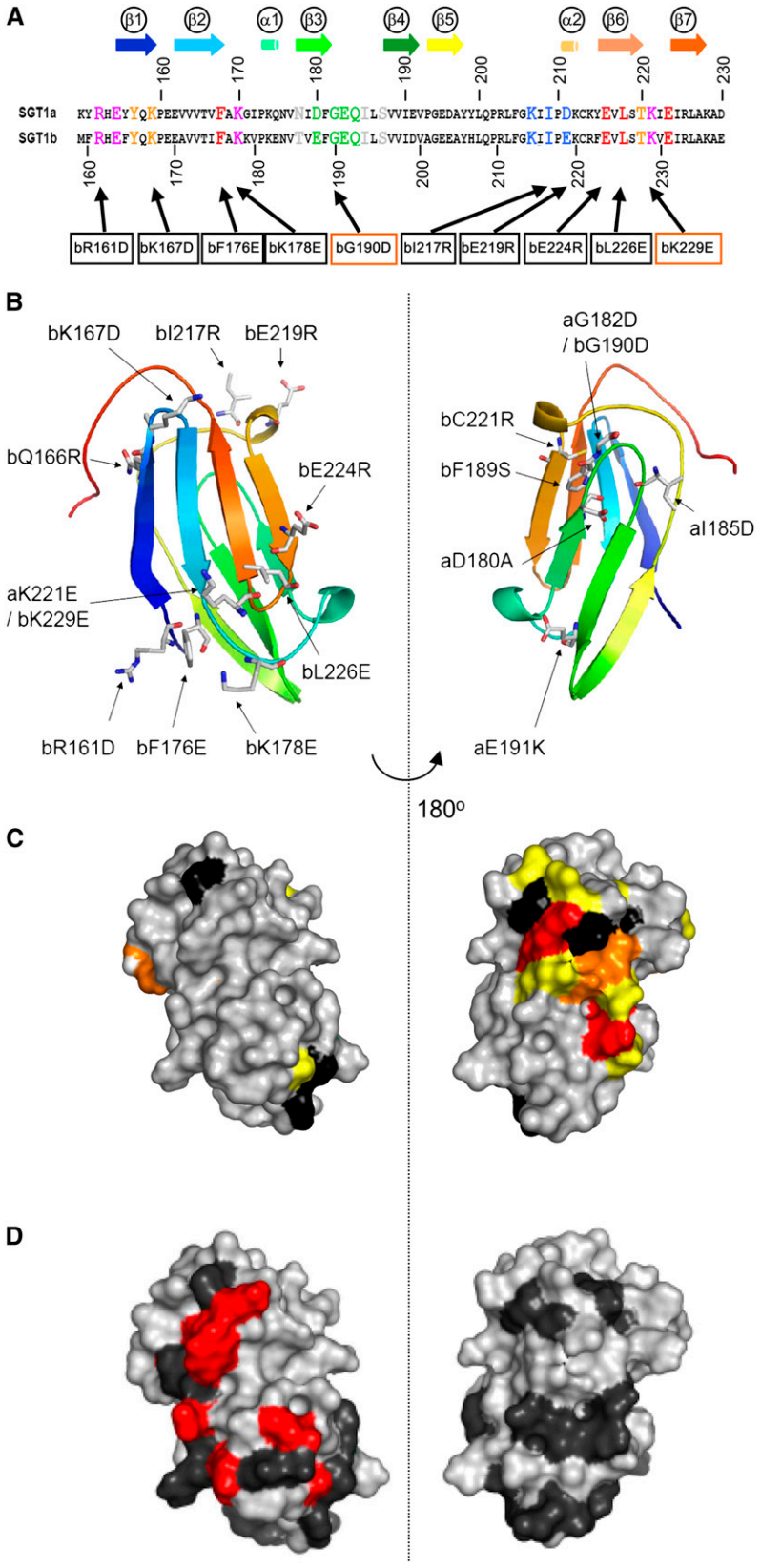

Figure 3. Structure and Interaction Surface Mapping of the CS Domain.

SGT1 was first isolated in plants as a RAR1-interacting protein in a yeast two-hybrid screen (Azevedo et al., 2002). However, the importance of the RAR1–SGT1 interaction for resistance has not been demonstrated previously. We tested whether bG190D and aG182D, which were unable to bind to At RAR1, could confer resistance. Functional analysis in *N. benthamiana* plants revealed that overexpression of these mutants confers Rx-mediated resistance (Figures 2 and 4D). Because silencing of Nb *SGT1* resulted in reduced steady state levels of Rx proteins (Azevedo et al., 2006), we tested whether overexpression of SGT1 derivatives can reverse the phenotype. As expected, transient expression of either At SGT1a or At SGT1b in Nb *SGT1*–silencing plants resulted in the recovery of Rx proteins compared with GUS controls (Figure 4E). Similar to the wild-type proteins, aG182D and bG190D were able to recover Rx proteins. These data suggest that SGT1 may not need RAR1, at least for this particular R protein, although we cannot exclude the possibility that weak, undetectable interactions between bG190D/aG182D and RAR1 may be enough for resistance when overexpressed.

The Conserved Surface of the CS Domain Binds to HSP90-NTD

To assess whether the association of HSP90 with the CS domain would compete with the binding of CHORD II, we performed an NMR titration of NTD (1:210) from Hv HSP90 on the ^{15}N-labeled CSa in the presence of the unlabeled CHORD II domain. Upon addition of increasing amounts of Hv HSP90-NTD in the absence of any nucleotides, some cross-peaks in the ^{1}H-^{15}N HSQC spectrum of the CS domain exhibited significant reductions in intensity (see Supplemental Figure 3C online), likely reflecting chemical exchange between the free and bound forms upon the addition of low amounts of Hv HSP90-NTD. These residues correspond to aE155, aY157, aQ158, aK159, aF168, aL218, and aL237, all of which cluster on one surface of CSa comprising β-sheets 1, 2, 6, and 7 (Figure 3D). Importantly, residues whose resonances were shifted upon binding of CHORD II were not perturbed by the addition of the Hv HSP90-NTD, suggesting that there is no overlap between the Hv HSP90-NTD and CHORD II binding sites.

There is a very good correlation between the region most perturbed upon the binding of Hv HSP90-NTD and those most conserved among SGT1 homologs. The conservation analysis shows that this face of the β-sheet including strands β1 and β2 is the most conserved (see Supplemental Figure 4 online). Several of the conserved residues around this area could not be probed by NMR due to signal overlap. However, given the similarity between the conservation pattern and the residues most affected in the NMR spectrum, the conserved pattern probably delineates the binding interface with HSP90. In summary, these data indicate that HSP90-NTD and CHORD II interact with the CS domain of SGT1 on opposite faces.

CS Domain Mutants That Abolish HSP90 Binding Are Not Able to Function in Rx Accumulation and Rx-Mediated Resistance

To further assess the role of the HSP90 interaction surface of SGT1 in disease resistance, we performed site-directed mutagenesis of CSb. Eight single amino acid substitutions spread over one face of the CS domain were made for residues that are either inside or outside the HSP90 binding region defined by the NMR data and the conservation profile (Figures 3A and 3B; see Supplemental Figure 4 online). The PVX-GFP assay in *N. benthamiana* plants showed that mutations bR161D, bK167D, bF176E, and bK178E resulted in LOF in Rx-mediated resistance against PVX-GFP (Figure 5A). By contrast, mutations bI217R, bE219R, bE224R, and bL226E did not affect At SGT1b function. Yeast two-hybrid and in vitro pull-down studies showed that all of the LOF mutations abolished binding to Hv HSP90, but those that were functional retained the interaction (Figure 5B; see Supplemental Figure 5 online). We also created the mutant aK221E in CSa, an equivalent of bK229E in CSb, to test the importance of the HSP90 interaction with At SGT1a in Rx resistance. Similar to bK229E, aK221E abolished the interaction with Hv HSP90-NTD and resulted in LOF in Rx resistance (Figures 5A and 5B). We did not detect any interaction between At SGT1a and Hv HSP90 in the yeast two-hybrid system (Figures 5C and 5B). However, using the in vitro pull-down assay, we found that At SGT1a interacts with Ta HSP90, but to a lesser extent than At SGT1b. The mutant aK221E was unable to interact with Ta HSP90 (Figure 5C). Together, the functionality of SGT1 in disease resistance tightly correlates with its HSP90 binding capability. Lastly, we tested whether these mutations affected the steady state levels of Rx protein. We found that transient expression of any HSP90 binding mutants, bK229E, aK221E, bR161D, bK167D, bF176E, and bK178E, confers weak recovery of Rx in Nb SGT1–silenced plants, but not to the levels accomplished by the wild-type protein or other CS mutants that bind to HSP90 (Figure 5D). These data strongly suggest that the interaction between HSP90 and

Figure 3. (continued).

(A) Amino acid sequence alignment of the CS domains of At SGT1a and At SGT1b along with their secondary structure. At SGT1b mutations isolated by LOF or DN screening are boxed in orange, whereas site-directed mutations are boxed in black.

(B) Three-dimensional map of the point mutations in the CSa and CSb domains. The ribbon representation of the CS domain of At SGT1a is shown in two opposing orientations.

(C) Amino acid residues affected in the presence of CHORD II highlighted on a surface representation. The affected residues are colored on the basis of the ^{1}H and ^{15}N chemical shift differences calculated between the bound and free forms. Red, orange, and yellow indicate large (0.3 ppm), medium (0.2 ppm), and small (0.1 ppm) differences, respectively. Black residues correspond either to Pro or to residues (Q184 and L204) whose signals disappeared upon titration.

(D) Amino acid residues significantly affected in the presence of Hv HSP90-NTD are shown in red. Black residues correspond either to Pro or to residues whose signal intensities could not be measured properly due to overlaps. **(C)** and **(D)** are drawn with pymol (DeLano, The PyMOL Molecular Graphics System; DeLano Scientific).

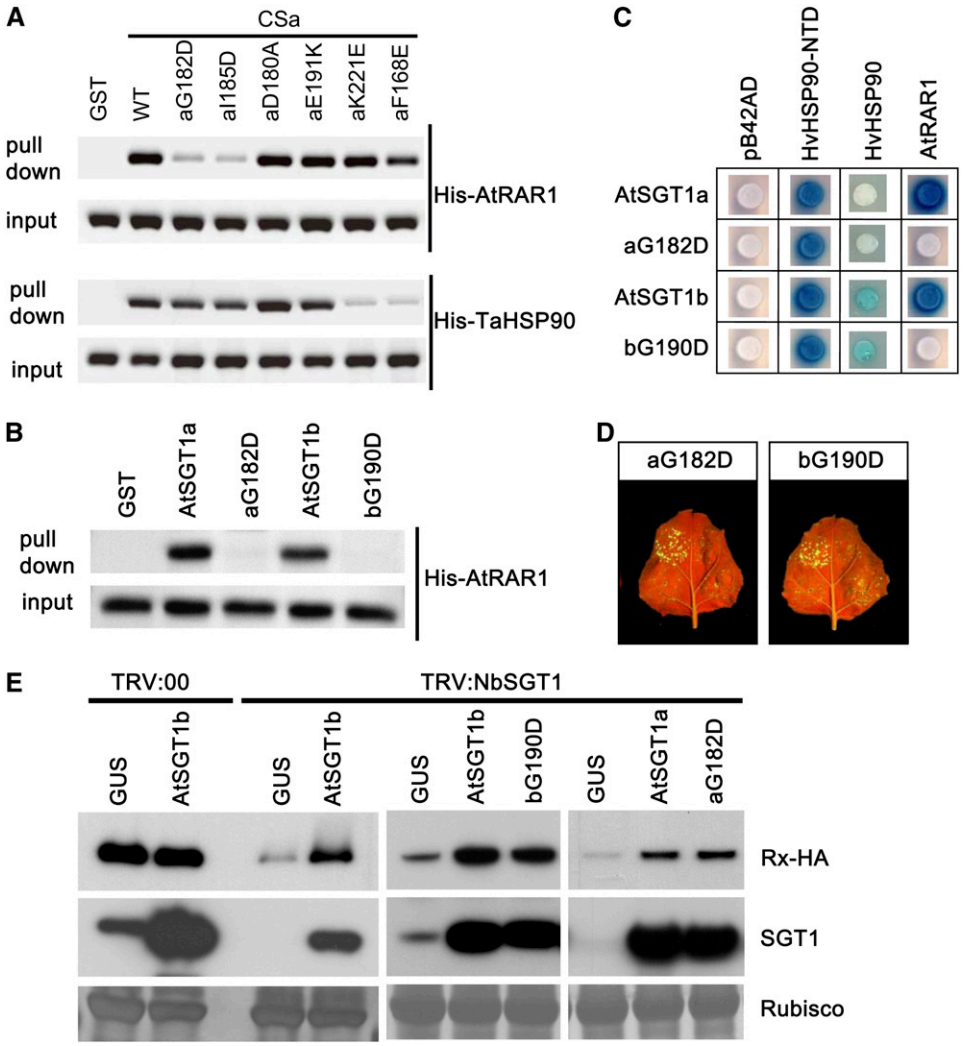

Figure 4. SGT1–RAR1 Interaction Is Not Required for Rx-Mediated Resistance.

(A) In vitro interaction assays. GST-tagged CSa (149 to 253), which was used for the NMR study, or its derivatives were incubated with purified At RAR1 and Ta HSP90 as indicated, and pull-down fractions were analyzed by SDS-PAGE followed by Coomassie blue staining.

(B) GST-tagged At SGT1a and GST-tagged At SGT1b or mutants were incubated with purified His_6-tagged At RAR1 as indicated, and pull-down fractions were analyzed by SDS-PAGE and Coomassie blue staining.

(C) Yeast two-hybrid analysis of the CS mutants. *Arabidopsis* SGT1 proteins and their derivatives were assayed for interaction with Hv HSP90-NTD and At RAR1 as shown in Figure 2.

(D) Functional assay of SGT1 mutants in Rx-mediated resistance against PVX. *Rx*-containing *N. benthamiana* plants silenced for Nb *SGT1* were coinfiltrated with *Agrobacterium* expressing wild-type At *SGT1a* or At *SGT1b* (bottom left; positive control) or its derivatives as indicated (right half of the leaves) or *GUS* (top left; negative control) together with *PVX-GFP*. Virus accumulation was monitored by GFP fluorescence under UV illumination at 5 d after inoculation.

(E) Rx restoration assay. Rx-HA–containing *N. benthamiana* plants silenced for Nb *SGT1* were coinfiltrated with *Agrobacterium* expressing wild-type At *SGT1a* or At *SGT1b* or its derivatives as indicated, and recovery of Rx protein levels was monitored at 6 d after inoculation by protein gel blotting using anti-HA antibody. SGT1 protein levels were monitored with SGSa (SGT1) antibody. Rubisco, ribulose-1,5-bis-phosphate carboxylase/oxygenase.

SGT1 is required for R protein accumulation to confer disease resistance.

HSP90, RAR1, and SGT1 Form a Ternary Complex in Vitro

The NMR experiments suggested that HSP90 and CHORD II may interact with the SGT1 CS domain on opposite faces simultaneously. To test this possibility we performed an in vitro pull-down assay with GST-tagged CHORD domains (Figure 6). As expected, Ta HSP90, but not At SGT1b, was pulled down by CHORD I in a binary control assay. Similarly, At SGT1b, but not Ta HSP90, was pulled down by CHORD II alone. The addition of At SGT1b did not affect the CHORD I–HSP90 interaction. However, in the presence of At SGT1b, Ta HSP90 was detected in the

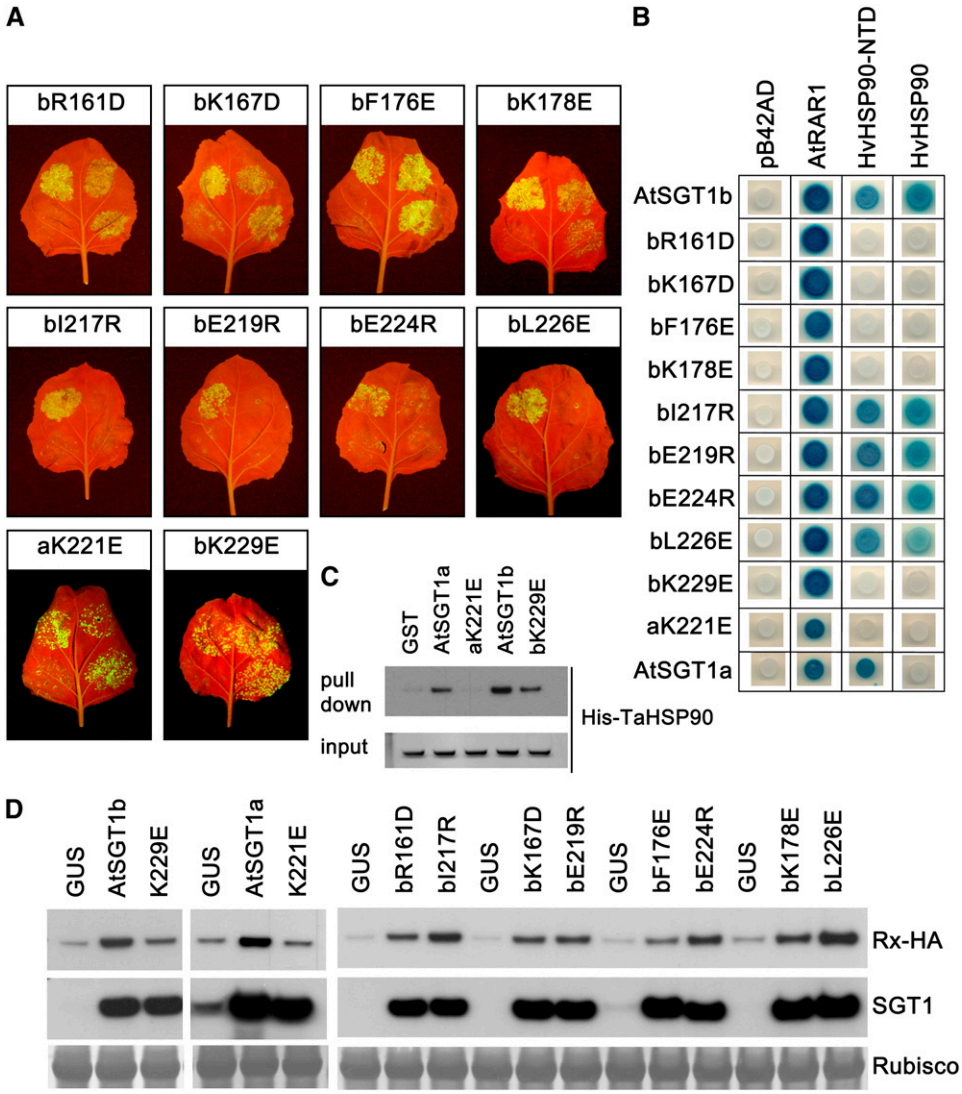

Figure 5. SGT1–HSP90 Interaction Is Required for SGT1 Function in Rx-Mediated Resistance.

(A) Functional assay of SGT1 mutants in Rx-mediated resistance against PVX. Functional assays were performed as shown in Figure 4D.

(B) Yeast two-hybrid analysis of the CS mutants. At SGT1b, At SGT1a, or their derivatives were assayed for interaction with At RAR1, Hv HSP90, or Hv HSP90-NTD by yeast two-hybrid analysis as shown in Figure 2.

(C) At SGTAa can interact with Ta HSP90 in vitro. N-terminal GST-tagged At SGT1a, At SGT1b, aK221E, and bK229E proteins were incubated with His_6-tagged HSP90. Pulled-down fractions were analyzed by SDS-PAGE and immunoblotting using anti-His_6 antibody.

(D) Rx restoration assay. Rx-HA–containing *N. benthamiana* plants silenced for Nb *SGT1* were coinfiltrated with *Agrobacterium* expressing wild-type At *SGT1a* or At *SGT1b* or its derivatives as indicated, and recovery of Rx protein levels was monitored at 6 d after inoculation by protein gel blot using anti-HA antibody. SGT1 protein levels were monitored with SGSa (SGT1) antibody. Rubisco, ribulose-1,5-bis-phosphate carboxylase/oxygenase.

CHORD II pull-down fraction. We conclude from these data that a TaHSP90-AtSGT1b-CHORD II ternary complex is able to form.

As both CHORD I and SGT1 interact with HSP90-NTD (Takahashi et al., 2003; this study), we next tested how CHORD I affects the association of SGT1 with HSP90. We found that increasing amounts of CHORD I compete against the interaction between At SGT1b and Ta HSP90 (Figure 7A). Thus CHORD I is likely to bind at or near the SGT1 interaction site of an HSP90 molecule. Next, we investigated how the full-length RAR1 protein affects the HSP90–SGT1 interaction. Surprisingly, the addition of At RAR1 to the AtSGT1b-TaHSP90 mixture resulted in a significant increase of Ta HSP90 pull-down with At SGT1b (Figure 7B). In addition, Ta HSP90 had no effect on the interaction of At SGT1b with At RAR1, suggesting that there is no competition between RAR1 and HSP90 for SGT1 binding. Increased levels of Ta HSP90 in the presence of At RAR1 were mostly dependent on the At SGT1b–At RAR1 interaction, as the addition of At RAR1 did not enhance the Ta HSP90–At SGT1b interaction when using

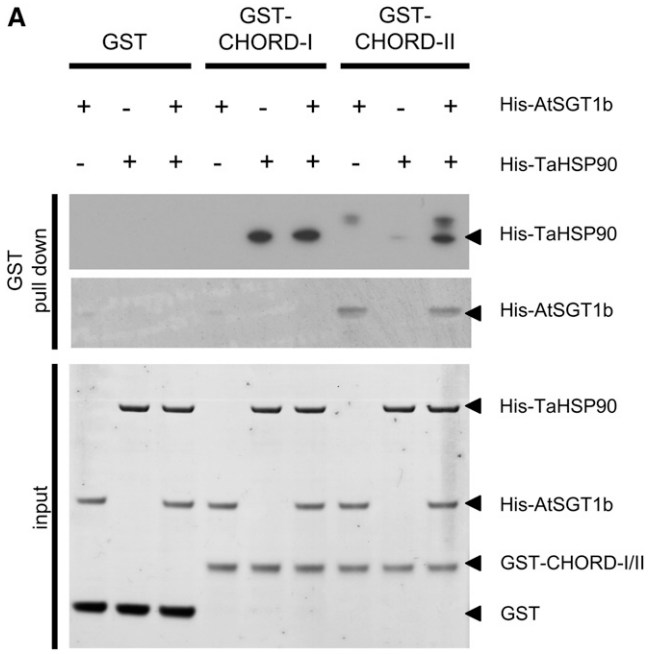

Figure 6. In Vitro Detection of the TaHSP90-AtSGT1b-CHORD II Complex.

GST-tagged CHORD I and GST-tagged CHORD II purified proteins were incubated with His_6-tagged At SGT1b and/or His_6-tagged Ta HSP90 as indicated. Pulled-down fractions were analyzed by SDS-PAGE and Coomassie blue staining for His_6-tagged At SGT1b detection or by immunoblotting using anti-His_6 antibody for His_6-tagged Ta HSP90 detection.

bG190D mutant (impaired in RAR1 binding). On the other hand, when pulled down with bK229E, which binds weakly to HSP90, the level of Ta HSP90 in the presence of At RAR1 was greatly reduced compared with that of the wild type. The residual amount of Ta HSP90 may be due to the weak binding activity of bK229E to Ta HSP90. These data strongly suggest that RAR1 enhances the HSP90–SGT1 interaction by associating with SGT1.

To further probe the effect of this interaction on the activity of HSP90, the ATPase activity of the full-length Ta HSP90 was measured using a regenerative ATPase assay. A weak activity of 0.18 ± 0.02 $\mu M \cdot min^{-1} \cdot \mu M^{-1}$ at 298K was measured for Ta HSP90 alone, in agreement with that previously measured for human and yeast HSP90s (Owen et al., 2002) (see Supplemental Figure 6 online). The rate of ATP hydrolysis of Ta HSP90 (concentration of 10 μM) was not altered in the presence of a large excess of CSa domain (concentration up to 100 μM) and/or of At RAR1 (up to 30 μM), suggesting that neither is able to modulate the ATPase activity of Ta HSP90 (analyzed at salt concentrations ranging from 10 to 150 mM). This is consistent with the previous report on yeast HSP90 that showed no modulation by full-length SGT1 (Catlett and Kaplan, 2006). Our data show that neither RAR1 nor the CS domain of SGT1 modulates HSP90 ATPase activity.

DISCUSSION

Interaction between SGT1 and HSP90 Is Required for Rx Resistance

Here, we present structural and functional characterization of the interaction between SGT1 and both RAR1 and HSP90, essential players in the disease resistance triggered by a number of R proteins. To define the interaction sites important for SGT1 function in resistance, we used two complementary approaches: (1) isolation of mutants through functional screening, and (2)

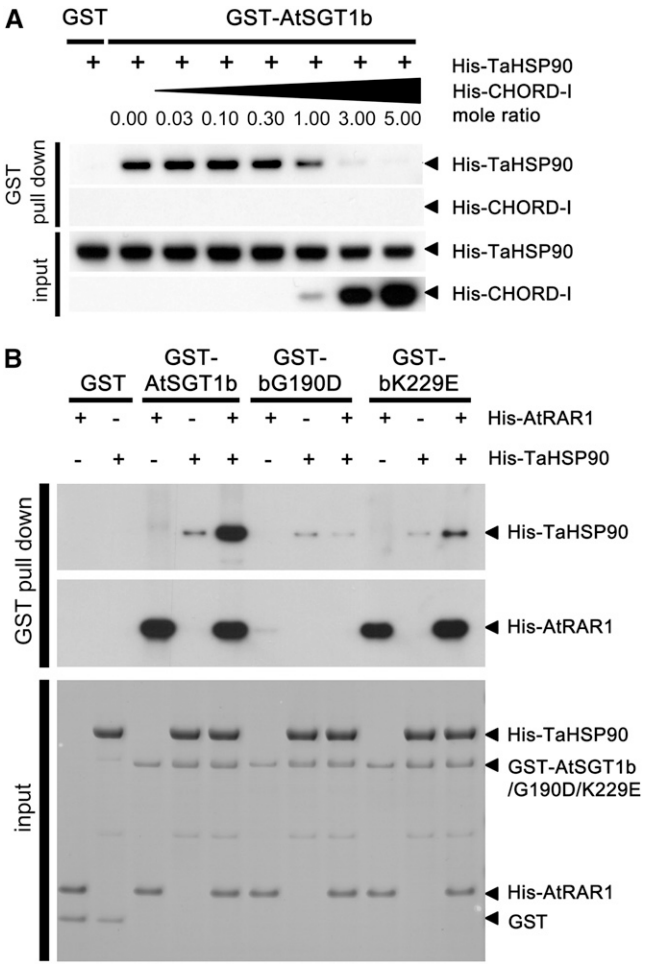

Figure 7. At RAR1 Complex Formation with At SGT1b and Ta HSP90 in Vitro.

(A) The CHORD I domain disrupts the AtSGT1b-TaHSP90 complex. GST-tagged At SGT1b was incubated with His_6-tagged Ta HSP90 in the absence or presence of increasing amounts of purified His_6-tagged CHORD I as indicated. GST pulled-down fractions were analyzed by SDS-PAGE and immunoblotting using anti-His_6 antibody.

(B) At RAR1 enhances the At SGT1b and Ta HSP90 interaction. GST-tagged At SGT1b and its derivatives were incubated with His_6-tagged Ta HSP90 and/or His_6-tagged At RAR1 as indicated. GST pulled-down fractions were analyzed by SDS-PAGE and immunoblotting using anti-His_6 antibody.

NMR-based structural modeling and interaction surface mapping. This combination of forward genetic screening and structural information proved to be a very powerful approach to drawing a fine interaction map. NMR titration experiments showed that the HSP90 interaction maps to β-strands 1 and 2 in the CS domain. Consistent with this, site-directed mutagenesis indicated that β-strands 1 and 2 are involved in the HSP90 interaction. Although bK229 is located between β-strands 6 and 7, it is very close to β-strands 1 and 2 in the structural model, which likely explains how the negative charge of the bK229E mutation disturbs the interaction with HSP90. A schematic representation of the combined NMR and mutational data on the isolated CS and Hv HSP90-NTD domains is shown in Figures 8A and 8C. There is excellent agreement between the region of the CS domain involved in Hv HSP90-NTD binding and the degree of sequence conservation (labeled red in Figure 8E). This further implies that regions of HSP90 outside of the HSP90-NTD domain are unlikely to contribute to the interaction with the CS domain, although these regions may affect the interaction with the full-length SGT1. Our results demonstrate that SGT1 function in Rx resistance is strictly dependent on its interaction with HSP90, indicating that a role of SGT1 may be to recruit chaperone activities to multiprotein assemblies.

CS and SGS Domains Are Required for Rx Resistance

Ninety-five percent of the mutations identified in our functional screening are located either in the CS or SGS domain, showing that these are required for Rx-mediated resistance. This is consistent with our recent finding that the TPR domain is dispensable for the resistance function of SGT1 but serves a regulatory role through the control of SGT1 stability in plants (Azevedo et al., 2006). In this context, it is intriguing that we found one DN mutation, bE119G, in TPRb. Transient expression of bE119G was able to recover Rx protein accumulation in Nb *SGT1*–silenced plants to similar levels as that conferred by wild-type At SGT1b (see Supplemental Figure 7 online). Similarly, bG190D was functional in the absence of endogenous SGT1 in Nb *SGT1*–silenced plants but exhibited DN activity in the presence of SGT1 in nonsilenced plants. These data support the idea that SGT1 may form higher order oligomers. Consistent with such a model, we recently described how plant SGT1 forms a TPR-mediated dimer that increases the stability of the protein in vitro (Nyarko et al., 2007).

We found that most DN mutations were localized in the SGSb domain. Moreover, most SGSb LOF mutants caused DN effects. Unlike bE119G, none of the DN mutants in SGSb was able to confer recovery of Rx protein accumulation to wild-type levels (see Supplemental Figure 7 online). The SGS domain is predicted to be the interaction domain for certain LRR proteins, including NBS-LRR proteins Mla1 from barley and human Nod1 (Dubacq et al., 2002; Bieri et al., 2004; da Silva Correia et al., 2007). Thus, we are currently investigating how these SGS mutations affect the formation and/or activation of R protein complexes. Given that the SGS domain may be involved in the interaction with HSP70 (Spiechowicz et al., 2007), it is tempting to speculate that SGT1 could act at an intermediate step of the HSP70/HSP90

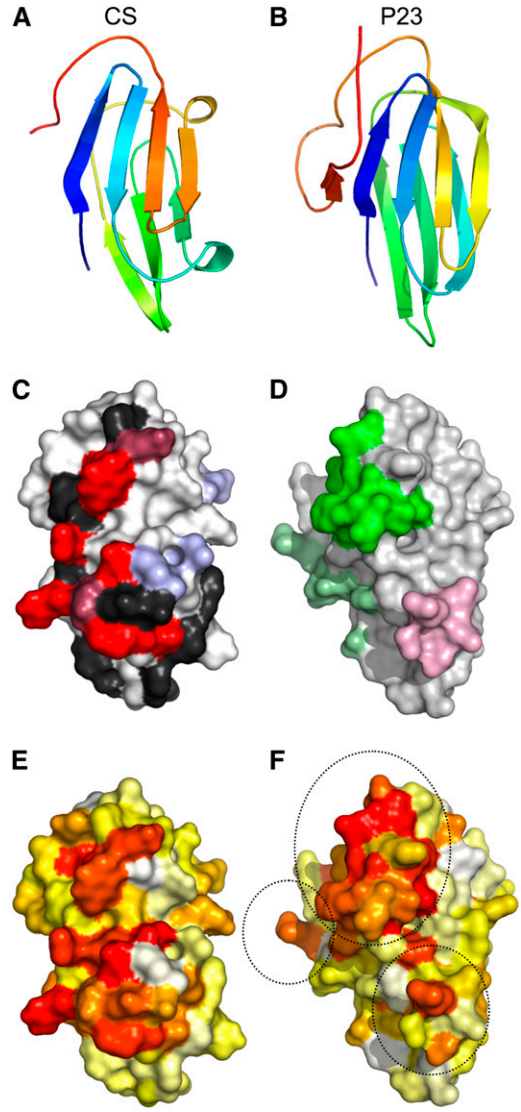

Figure 8. Similarities and Difference between P23 and SGT1.

(A) and **(B)** Ribbon representation of CS **(A)** and P23 **(B)** domains showing the orientations of the surfaces below.

(C) Combined analysis from the NMR and the mutagenesis results on the CS domain showing the residues involved in the interaction with HSP90-NTD (red and dark red). Red positions correspond to residues found by either NMR or mutagenesis, and dark red positions correspond to residues found by both techniques. Light blue positions correspond to those mutations that had no effect on the SGT1–HSP90 interaction. Black positions indicate residues that could not be probed by NMR.

(D) P23 interacts with HSP90 at three points: the middle domain (shown in green) and the NTD (light green) of a HSP90 monomer as well as the NTD of the other HSP90 monomer (light pink) (Ali et al., 2006).

(E) and **(F)** Conserved amino acid residues in SGT1 **(E)** and P23 **(F)** calculated using the Rate4site algorithm (Pupko et al., 2002). Colors from red to white indicate the most conserved to the most variable positions.

chaperone cycle, ensuring proper client loading between HSP70 and HSP90.

Differential Modes of HSP90 Binding by the SGT1 CS Domain and P23

Although this and other studies have shown that the CS domain is structurally similar to cochaperone P23 (Lee et al., 2004) (Figures 8A and 8B), our data suggest that they have distinct modes of binding to HSP90. The recent crystal structure of full-length HSP90 in a closed conformation bound to Sba1p, the yeast homolog of P23, revealed three interaction sites (Figure 8D): the middle domain (shown in green) and the N-terminal domain of an HSP90 monomer (light green) as well as the N-terminal domain of the other HSP90 monomer (light pink) (Ali et al., 2006). The last strand of P23 makes extensive contacts with the middle domain of HSP90. However, the CS domain of SGT1 does not have an equivalent strand and thus cannot engage in the same interaction (see Supplemental Figure 8 online). Moreover, there is a tight equivalence between the CS conservation pattern and the experimentally defined binding interface with HSP90, suggesting that, in contrast with P23, the binding of the CS domain to HSP90 is restricted to the N-terminal domain of HSP90.

RAR1 and SGT1 Do Not Modulate the ATPase Activity of HSP90 in Vitro

To investigate further the role of SGT1 and RAR1 in HSP90 function, we measured the ATPase activity of Ta HSP90 and found that neither the CS domain of At SGT1a nor At RAR1, alone or combined, is able to modulate the ATPase activity of Ta HSP90. This is consistent with a previous report on yeast HSP90 that showed no modulation by SGT1 (Catlett and Kaplan, 2006). In this sense, SGT1 and RAR1 are quite different from the majority of the other known cochaperones that interact with HSP90-NTD. For example, the cochaperone AHA1 stimulates HSP90 ATPase activity (Panaretou et al., 2002), while P23, CDC37, and STI1 behave as inhibitors (Prodromou et al., 1999; Siligardi et al., 2002, 2004; Richter et al., 2003). All have been shown to modulate HSP90 activity in vitro even in the absence of any client protein/complex. Other known cochaperones that bind HSP90 without any activity, such as CPR6, can in fact modulate other cochaperone activity (Prodromou et al., 1999). Therefore, the potential for competition between SGT1 and RAR1 with other cochaperones remains an important question for future studies.

RAR1 Functions to Enhance the HSP90–SGT1 Interaction

Structural analysis combined with mutational and biochemical assays showed that CHORD II and HSP90-NTD interact physically with opposite faces of the CS domain, allowing the formation of a ternary complex. Here, we postulate a model suggesting how these three proteins may interact and function. First, it is clear that SGT1 is able to interact directly with HSP90 even in the absence of RAR1 (Figure 9A), as shown by the yeast two-hybrid analysis and in vitro pull-down assays. Consistent with this, SGT1 interacts with HSP90 in yeast, which does not contain any RAR1 homologs (Bansal et al., 2004). The fact that the HSP90 interaction surface of the CS domain, but not that of RAR1, is highly conserved in eukaryotes also supports this notion. This interaction should occur between the CS domain and HSP90-NTD. In *rar1* mutants, R protein levels are reduced, but not completely (Tornero et al., 2002; Bieri et al., 2004; Holt et al., 2005). Thus, in the absence of RAR1, R proteins can accumulate as a consequence of the HSP90–SGT1 interaction (Azevedo et al., 2006). Consistent with this, reduction of both RAR1 and SGT1 levels results in additive susceptibility for some R proteins (Austin et al., 2002; Azevedo et al., 2002). Thus, while the RAR1–SGT1 interaction is not required for resistance triggered by some R proteins (Figure 4) (Bieri et al., 2004), the SGT1–HSP90 interaction is essential (Figure 5) (Peart et al., 2002). In the

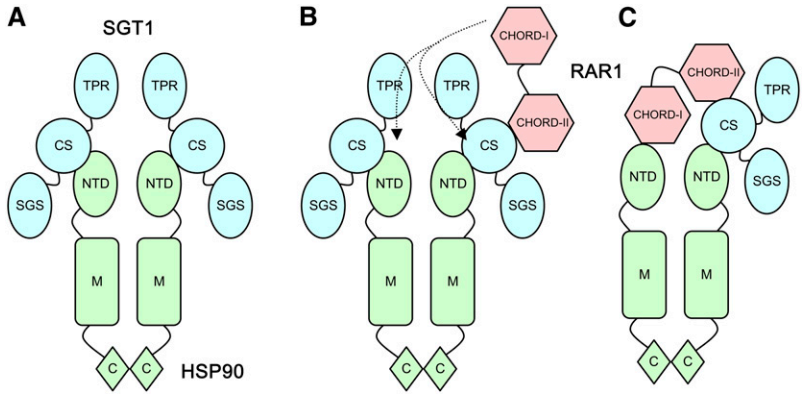

Figure 9. Hypothetical Model for the HSP90–RAR1–SGT1 Interaction.

(A) SGT1 (light blue) can associate with HSP90 (light green) via the NTD–CS interaction independently of RAR1. Note that HSP90 functions as a dimer.
(B) RAR1 (light pink) can interact with SGT1 via the CS–CHORD II interaction. As CHORD I can also interact with either HSP90 monomer, this complex may be a transient form.
(C) CHORD I can out-compete SGT1 from the HSP90 monomer, but the ternary complex is maintained in a more stable conformation.

presence of RAR1, the CS domain of SGT1 can simultaneously associate with HSP90-NTD and the CHORD II domain of RAR1 (Figures 6 and 9B). However, CHORD I can also interact with NTD of either HSP90 monomer (Figure 6). Because CHORD I alone competes off the CS domain from HSP90-NTD, but RAR1 cannot, it is likely that CHORD I interacts with the other HSP90 monomer (Figure 9C). Since RAR1 enhances the interaction between SGT1 and HSP90 (Figure 7B), it is likely to stabilize the SGT1-HSP90 binary complex by holding the two proteins simultaneously. At this point, we cannot explain how At RAR1 and At SGT1b function additively for some R proteins but antagonistically for other R proteins (Austin et al., 2002; Holt et al., 2005). As CHORD I can compete off SGT1 from HSP90, in some cases RAR1 might interfere with certain function(s) of SGT1. Thus, a fine balance between RAR1 and SGT1 on HSP90 is crucial to determine the fate of an R protein. Further biochemical reconstitution experiments with client proteins and other cochaperones and in vivo assay systems are obviously needed to fully elucidate the function of this unique chaperone complex.

METHODS

Plant Materials, Bacteria, and Virus Strains

Transgenic *Nicotiana benthamiana* plants carrying *Rx*, *N*, and *Pto* resistance genes (Superbenth line), their growth conditions, and PVX-GFP were described previously (Peart et al., 2002). Transgenic *N. benthamiana* plants expressing Rx-HA under the control of its own promoter were described elsewhere (Azevedo et al., 2006). Details of virus induced gene silencing together with *Agrobacterium tumefaciens*–mediated transient expression were described previously (Azevedo et al., 2006). All work involving virus-infected material was performed in containment glasshouses under Department for Environment Food and Rural Affairs license PHL 161A14178.

Random and Site-Specific Mutagenesis of *Arabidopsis SGT1b*

The *Arabidopsis thaliana* (At) *SGT1b* open reading frame was amplified and mutagenized by an error-prone PCR method before cloning into pBIN61 in *Agrobacterium* strain C58C1 carrying plasmid pCH32, used for transient gene expression under the control of the 35S promoter in planta (Bendahmane et al., 2002). For LOF screening, At *SGT1b* mutants were coexpressed with PVX-GFP by *Agrobacterium* (OD = 0.3 and 0.001) in *Rx*-containing *N. benthamiana* plants silenced for Nb *SGT1*. After 4 to 7 d, PVX-GFP accumulation was monitored by GFP fluorescence under UV light. LOF mutants were sequenced, and causative mutations were identified. When multiple mutations were found, single mutations were split by chimeric PCR and causative mutations were identified by retesting single mutations in *N. benthamiana* plants. For DN screening, At *SGT1b* mutants were coexpressed with pB1Rx (Bendahmane et al., 2002) and PVX-GFP (OD = 0.15, 0.15, and 0.001, respectively) in *N. benthamiana* wild-type plants, and necrotic spots were monitored at 5 to 7 d after infiltration.

Yeast Two-Hybrid Analysis

At *SGT1b* wild-type and mutant open reading frames were amplified by PCR and cloned in pLexA (Clontech) for the yeast two-hybrid experiments. At RAR1, At HSP90.1, Hv HSP90 (97% similar to At HSP90.1; from barley [*Hordeum vulgare*]), and Hv HSP90-NTD clones in pB42AD were described previously (Takahashi et al., 2003). Site-directed mutagenesis was performed using AtSGT1b-pGEX-6P-1 constructs. Interaction analyses were performed as described in the manufacturer's protocol (Matchmaker LexA two-hybrid system; Clontech).

Gene Expression and Protein Purification from *Escherichia coli*

DNA fragments encoding CSa (residues 149 to 253), CHORD II (residues 141 to 224), or Hv HSP90-NTD (residues 1 to 210) were used to create His_6 or His_6/GST fusion proteins in pETM11 or pETM30 expression vector, respectively (Gunter Stier, EMBL). His_6-tagged Ta HSP90 was kindly provided by Adina Breiman (Tel Aviv University). We chose Ta HSP90 for in vitro binding assays because of its higher solubility compared with Hv HSP90 (99.7% amino acid similarity). Soluble His_6-tagged GST fusion proteins were immobilized on GSH agarose (Sigma-Aldrich). The beads were washed by applying 5 volumes of 1 M NaCl buffer, equilibrated with 5 volumes of 50 mM phosphate, pH 8.0, and eluted with 50 mM phosphate buffer, pH 8.0, and 10 mM GSH (Sigma-Aldrich). They were cleaved using His_6-tagged tobacco etch virus (TEV) protease (1% [w/w] protease/fusion protein) overnight at room temperature. His_6-tagged TEV protease and the His_6-tagged GST were then removed using nickel-nitrilotriacetic acid agarose resin. Purified samples were exchanged into appropriate buffers and concentrated using a Cell Amicon (Millipore) system with YM-type membranes with cutoff adapted to each of the domain sizes. DNA fragments expressing full-length At SGT1a, aG182D, At SGT1b, or bK229E were cloned into *Eco*RI and *Not*I sites of pGEX-6P-1 (Amersham Pharmacia Biotech). GST fusion proteins were expressed and purified from *E. coli* BL21 cells according to the manufacturer's protocol (Amersham Pharmacia Biotech). His_6-TEV-AtRAR1 was expressed and purified according to the manufacturer's protocol (Novagen).

NMR Spectroscopy

The CSa domain uniformly labeled with ^{15}N or $^{13}C/^{15}N$ was prepared using M9 minimal growth medium supplemented with ^{15}N-labeled ammonium chloride and ^{13}C-labeled glucose. NMR experiments were performed on a Brucker Avance 600 spectrometer equipped with a triple resonance probe at 293K. NMR experiments for resonance assignment and structure determination were performed at a protein concentration of 0.5 mM. The sequential backbone resonance assignments were achieved using standard ^{15}N-^{1}H HSQC, HNCA, CBCA(CO)NH, HBHA(CO)NH, NOESY-HSQC, and TOSCY-HSQC experiments. Proton chemical shifts (ppm) were referenced relative to internal 2,2-dimethyl-2-silapentane-5-sulfonic acid, and ^{15}N and ^{13}C references were set indirectly relative to 2,2-dimethyl-2-silapentane-5-sulfonic acid using frequency ratio. The NMR chemical shift perturbation assays were performed using ^{15}N-labeled CSa domain (149 to 253) and unlabeled CHORD II (141 to 224) or Hv HSP90-NTD (1 to 210) at 293K. The initial NMR samples contained 0.1 mM ^{15}N-labeled CSa (20 mM NaH_2PO_4, pH 5.5, 150 mM NaCl, 2 mM DTT, and 10 μM $ZnCl_2$). A concentrated CHORD II (0.2 mM) sample diluted in the same buffer was added to ^{15}N-labeled CSa with the ratio adjusted from 0 to 1. The same experiments in a different buffer (40 mM NaH_2PO_4, pH 7, 50 mM NaCl, and 5 mM DTT) were performed with CSa titrated with a concentrated solution of Hv HSP90-NTD (1.5 mM). Last, a preformed complex of ^{15}N-labeled CSa and unlabeled CHORD II domains (2.5 mM) was titrated with Hv HSP90-NTD (1.5 mM) in the same buffers as in the CSa/Hv HSP90-NTD titration experiment. The perturbations were monitored by acquisition of ^{15}N-^{1}H HSQC spectra. To monitor the binding region of Hv HSP90-NTD onto the CSa/CHORD II complex, we quantitatively identified the cross-peaks broadening at the lowest ratios of NTD to CSa by measuring the ratio between the cross-peak intensities at the beginning (I_{free}) and along the titration (I). The log of I_{free}/I was found to vary linearly with the concentration of the Hv HSP90-NTD domain, and the fitted slope was used to define the rate of broadening for each cross-peak

(based on five titration points). From the ensemble of measured rates of broadening, the residues whose rates of broadening were 1 SD above the mean rate of broadening were considered significantly perturbed.

Pull-Down Assays

Ten micrograms of the GST fusion protein was incubated with 10 μg of His_6-tagged protein in PDB (20 mM HEPES-KOH, pH 7.5, 50 mM KCl, 2.5 mM $MgCl_2$, 0.2% Nonidet P-40, 1 mM DTT, and 100 μM phenylmethylsulfonyl fluoride) at 4°C. After 1 h, the GST fusion protein was pulled down using 50% glutathione–Sepharose 4 FF (Amersham), washed three times with PDB, and eluted with 10 mM GSH. His_6-tagged bound proteins were analyzed by SDS-PAGE and Coomassie Brilliant Blue staining or immunoblotting as indicated.

Antibodies

The polyclonal antibodies against SGSa from At SGT1a and Hv HSP90-NTD were described previously (Takahashi et al., 2003; Azevedo et al., 2006). Anti-His_6 antibody was obtained from Novagen. Anti-HA antibody was obtained from Roche, and anti-GST antibody was obtained from Upstate.

ATPase Activity

HSP90 ATPase activities were measured using a regenerative ATPase assay as described previously (Ali et al., 1993). Assays were performed at 25°C in a buffer containing 50 mM Tris, pH 7, tested with gradient from 10 to 150 mM KCl, 5 mM $MgCl_2$, 2 mM DTT, and 10 μM $ZnCl_2$, with 1 mM ATP added in a 1-mL stirred cell. Protein concentrations were 10 μM for Ta HSP90, 5 to 100 μM for CSa, and 5 to 30 μM for At RAR1. Absence of any contaminating ATPase activity was obtained with pure proteins (>95%) after three purifications steps (Richter et al., 2001). Full and specific inactivation of the ATPase of HSP90 was obtained with geldanamycin (Sigma-Aldrich) at a concentration of 20 μM.

Accession Numbers

Sequence data from this article can be found in the Arabidopsis Genome Initiative database or GenBank under the following accession numbers: At RAR1 (At5g51700), At SGT1a (At4g23570), At SGT1b (At4g11260), At HSP90.1 (At5g52640), and Hv HSP90 (AY325266).

Supplemental Data

The following materials are available in the online version of this article.

Supplemental Figure 1. Protein Blot Analysis of At SGT1b and Its Derivatives Expressed Transiently in *N. benthamiana*.

Supplemental Figure 2. RNA Gel Blot Analysis of PVX mRNA in the DN Mutant.

Supplemental Figure 3. NMR Analysis of CSa.

Supplemental Figure 4. Conserved Amino Acid Residues in SGT1 Proteins Calculated Using the Rate4site Algorithm.

Supplemental Figure 5. In Vitro Pull-Down Analysis of SGT1 Derivatives.

Supplemental Figure 6. ATPase Activity Assay for Ta HSP90.

Supplemental Figure 7. Expression Levels of TPRb and SGSb Mutants and Their Effects on Rx Restoration Capability.

Supplemental Figure 8. Probing the Absence of Any C-Terminal Strand as in P23 Structure.

ACKNOWLEDGMENTS

We thank Adina Breiman for providing Ta *HSP90* cDNA clone and Mary Antypa for technical support. We are grateful to F. Toma and P. Curmi for giving us access to the 600-MHz NMR spectrometer at Evry University. This work was funded by grants from the Biotechnology and Biological Science Research Council (G.M., C.K., and K.S.), the Gatsby Foundation (K.S.), and the Japan Society for the Promotion of Science (K.S.). B.A., M.B., and Y.K. were supported by the Délégation Générale pour l'Armement, Marie Curie Fellowship Program, and the Japan Society for the Promotion of Science, respectively.

Received January 15, 2007; revised October 7, 2007; accepted October 31, 2007; published November 21, 2007.

REFERENCES

Ali, J.A., Jackson, A.P., Howells, A.J., and Maxwell, A. (1993). The 43-kilodalton N-terminal fragment of the DNA gyrase-B protein hydrolyzes ATP and binds coumarin drugs. Biochemistry **32:** 2717–2724.

Ali, M.M.U., Roe, S.M., Vaughan, C.K., Meyer, P., Panaretou, B., Piper, P.W., Prodromou, C., and Pearl, L.H. (2006). Crystal structure of an Hsp90-nucleotide-p23/Sba1 closed chaperone complex. Nature **440:** 1013–1017.

Austin, M.J., Muskett, P., Kahn, K., Feys, B.J., Jones, J.D., and Parker, J.E. (2002). Regulatory role of *SGT1* in early *R* gene-mediated plant defenses. Science **295:** 2077–2080.

Azevedo, C., Betsuyaku, S., Peart, J., Takahashi, A., Noel, L., Sadanandom, A., Casais, C., Parker, J., and Shirasu, K. (2006). Role of SGT1 in resistance protein accumulation in plant immunity. EMBO J. **25:** 2007–2016.

Azevedo, C., Sadanandom, A., Kitagawa, K., Freialdenhoven, A., Shirasu, K., and Schulze-Lefert, P. (2002). The RAR1 interactor SGT1, an essential component of *R* gene-triggered disease resistance. Science **295:** 2073–2076.

Bansal, P.K., Abdulle, R., and Kitagawa, K. (2004). Sgt1 associates with Hsp90: An initial step of assembly of the core kinetochore complex. Mol. Cell. Biol. **24:** 8069–8079.

Bendahmane, A., Farnham, G., Moffett, P., and Baulcombe, D.C. (2002). Constitutive gain-of-function mutants in a nucleotide binding site-leucine rich repeat protein encoded at the Rx locus of potato. Plant J. **32:** 195–204.

Bieri, S., Mauch, S., Shen, Q.H., Peart, J., Devoto, A., Casais, C., Ceron, F., Schulze, S., Steinbiss, H.H., Shirasu, K., and Schulze-Lefert, P. (2004). RAR1 positively controls steady state levels of barley MLA resistance proteins and enables sufficient MLA6 accumulation for effective resistance. Plant Cell **16:** 3480–3495.

Catlett, M.G., and Kaplan, K.B. (2006). Sgt1p is a unique co-chaperone that acts as a client adaptor to link Hsp90 to Skp1p. J. Biol. Chem. **281:** 33739–33748.

Cornilescu, G., Delaglio, F., and Bax, A. (1999). Protein backbone angle restraints from searching a database for chemical shift and sequence homology. J. Biomol. NMR **13:** 289–302.

da Silva Correia, J.D., Miranda, Y., Leonard, N., and Ulevitch, R. (2007). SGT1 is essential for Nod1 activation. Proc. Natl. Acad. Sci. USA **104:** 6764–6769.

Dubacq, C., Guerois, R., Courbeyrette, R., Kitagawa, K., and Mann, C. (2002). Sgt1p contributes to cyclic AMP pathway activity and physically interacts with the adenylyl cyclase Cyr1p/Cdc35p in budding yeast. Eukaryot. Cell **1:** 568–582.

Garcia-Ranea, J.A., Mirey, G., Camonis, J., and Valencia, A. (2002). p23 and HSP20/alpha-crystallin proteins define a conserved sequence domain present in other eukaryotic protein families. FEBS Lett. **529:** 162–167.

Ginalski, K. (2006). Comparative modeling for protein structure prediction. Curr. Opin. Struct. Biol. **16:** 172–177.

Gray, W.M., Muskett, P.R., Chuang, H.-W., and Parker, J.E. (2003). The Arabidopsis SGT1b protein is required for SCFTIR1-mediated auxin response. Plant Cell **15:** 1310–1319.

Heise, C.T., Le Duff, C.S., Boter, M., Casais, C., Airey, J.E., Leech, A.P., Amigues, B., Guerois, R., Moore, G.R., Shirasu, K., and Kleanthous, C. (2007). Biochemical characterisation of RAR1 CHORD domains, a novel class of zinc-dependent protein-protein interaction modules. Biochemistry **46:** 1612–1623.

Holt, B.E., Belkhadir, Y., and Dangl, J.L. (2005). Antagonistic control of disease resistance protein stability in the plant immune system. Science **309:** 929–932.

Hubert, D.A., Tornero, P., Belkhadir, Y., Krishna, P., Takahashi, A., Shirasu, K., and Dangl, J.L. (2003). Cytosolic HSP90 associates with and modulates the *Arabidopsis* RPM1 disease resistance protein. EMBO J. **22:** 5679–5689.

Jones, J.D.G., and Dangl, J.L. (2006). The plant immune system. Nature **444:** 323–329.

Kanzaki, H., Saitoh, A., Ito, S., Fujisawa, S., Kamoun, S., Katou, S., Yoshioka, H., and Terauchi, R. (2003). Cytosolic HSP90 and HSP70 are essential components of INF1-mediated hypersensitive response and non-host resistance to *Pseudomonas cihorii* in *Nicotiana benthamiana*. Mol. Plant Pathol. **4:** 383–391.

Kitagawa, K., Skowyra, D., Elledge, S.J., Harper, J.W., and Hieter, P. (1999). *SGT1* encodes an essential component of the yeast kinetochore assembly pathway and a novel subunit of the SCF ubiquitin ligase complex. Mol. Cell **4:** 21–33.

Lee, Y.T., Jacob, J., Michowski, W., Nowotny, M., Kuznicki, J., and Chazin, W.J. (2004). Human Sgt1 binds HSP90 through the CHORD-Sgt1 domain and not the tetratricopeptide repeat domain. J. Biol. Chem. **279:** 16511–16517.

Lingelbach, L.B., and Kaplan, K.B. (2004). The interaction between Sgt1p and Skp1p is regulated by HSP90 chaperones and is required for proper CBF3 assembly. Mol. Cell. Biol. **24:** 8938–8950.

Liu, Y.L., Burch-Smith, T., Schiff, M., Feng, S.H., and Dinesh-Kumar, S.P. (2004). Molecular chaperone Hsp90 associates with resistance protein N and its signaling proteins SGT1 and Rar1 to modulate an innate immune response in plants. J. Biol. Chem. **279:** 2101–2108.

Niikura, Y., Ohta, S., Vandenbeldt, K.J., Abdulle, R., McEwen, B.F., and Kitagawa, K. (2006). 17-AAG, an Hsp90 inhibitor, causes kinetochore defects: A novel mechanism by which 17-AAG inhibits cell proliferation. Oncogene **25:** 4133–4146.

Nyarko, A., Mosbahi, K., Rowe, A.J., Botar, M., Shirasu, K., and Kleanthous, C. (2007). TPR-mediated self-association of plant Sgt1. Biochemistry **46:** 11331–11341.

Owen, B.A.L., Sullivan, W.P., Felts, S.J., and Toft, D.O. (2002). Regulation of heat shock protein 90 ATPase activity by sequences in the carboxyl terminus. J. Biol. Chem. **277:** 7086–7091.

Panaretou, B., et al. (2002). Activation of the ATPase activity of Hsp90 by the stress-regulated cochaperone Aha1. Mol. Cell **10:** 1307–1318.

Pearl, L.H., and Prodromou, C. (2006). Structure and mechanism of the Hsp90 molecular chaperone machinery. Annu. Rev. Biochem. **75:** 271–294.

Peart, J.R., et al. (2002). The ubiquitin ligase-associated protein SGT1 is required for host and nonhost disease resistance in plants. Proc. Natl. Acad. Sci. USA **99:** 10865–10869.

Pratt, W.B., and Toft, D.O. (2003). Regulation of signaling protein function and trafficking by the hsp90/hsp70-based chaperone machinery. Exp. Biol. Med. **228:** 111–133.

Prodromou, C., Siligardi, G., O'Brien, R., Woolfson, D.N., Regan, L., Panaretou, B., Ladbury, J.E., Piper, P.W., and Pearl, L.H. (1999). Regulation of Hsp90 ATPase activity by tetratricopeptide repeat (TPR)-domain co-chaperones. EMBO J. **18:** 754–762.

Pupko, T., Bell, R.E., Mayrose, I., Glaser, F., and Ben-Tal, N. (2002). Rate4Site: An algorithmic tool for the identification of functional regions in proteins by surface mapping of evolutionary determinants within their homologues. Bioinformatics **18** (suppl.): S71–S77.

Richter, K., Muschler, P., Hainzl, O., and Buchner, J. (2001). Coordinated ATP hydrolysis by the Hsp90 dimer. J. Biol. Chem. **276:** 33689–33696.

Richter, K., Muschler, P., Hainzl, O., Reinstein, J., and Buchner, J. (2003). Sti1 is a non-competitive inhibitor of the Hsp90 ATPase. Binding prevents the N-terminal dimerization reaction during the ATPase cycle. J. Biol. Chem. **278:** 10328–10333.

Sadanandom, A., Findlay, K., Doonan, J.H., Schulze-Lefert, P., and Shirasu, K. (2004). CHPA, a cysteine- and histidine-rich-domain-containing protein, contributes to maintenance of the diploid state in *Aspergillus nidulans*. Eukaryot. Cell **3:** 984–991.

Shirasu, K., Lahaye, L., Tan, M.-W., Zhou, F., Azevedo, C., and Schulze-Lefert, P. (1999). A novel class of eukaryotic zinc-binding protein is required for disease resistance signaling in barley and development in *C. elegans*. Cell **99:** 355–366.

Shirasu, K., and Schulze-Lefert, P. (2000). Regulators of cell death in disease resistance. Plant Mol. Biol. **44:** 371–385.

Siligardi, G., Hu, B., Panaretou, B., Piper, P.W., Pearl, L.H., and Prodromou, C. (2004). Co-chaperone regulation of conformational switching in the Hsp90 ATPase cycle. J. Biol. Chem. **279:** 51989–51998.

Siligardi, G., Panaretou, B., Meyer, P., Singh, S., Woolfson, D.N., Piper, P.W., Pearl, L.H., and Prodromou, C. (2002). Regulation of Hsp90 ATPase activity by the co-chaperone Cdc37p/p50(cdc97). J. Biol. Chem. **277:** 20151–20159.

Spiechowicz, M., Zylicz, A., Bieganowski, P., Kuznicki, J., and Filipek, A. (2007). Hsp70 is a new target of Sgt1—An interaction modulated by S100A6. Biochem. Biophys. Res. Commun. **357:** 1148–1153.

Steensgaard, P., Garre, M., Muradore, I., Transidico, P., Nigg, E.A., Kitagawa, K., Earnshaw, W.C., Faretta, M., and Musacchio, A. (2004). Sgt1 is required for human kinetochore assembly. EMBO Rep. **5:** 626–631.

Takahashi, A., Casais, C., Ichimura, K., and Shirasu, K. (2003). HSP90 interacts with RAR1 and SGT1, and is essential for RPS2-mediated resistance in *Arabidopsis*. Proc. Natl. Acad. Sci. USA **100:** 11777–11782.

Tornero, P., Merritt, P., Sadanandom, A., Shirasu, K., Innes, R.W., and Dangl, J.L. (2002). *RAR1* and *NDR1* contribute quantitatively to disease resistance in Arabidopsis, and their relative contributions are dependent on the *R* gene assayed. Plant Cell **14:** 1005–1015.